Photoluminescence, stimulated and laser emission in $CuInSe_2$ crystals

I.E. Svitsiankou[1], V.N. Pavlovskii[1], E.V. Lutsenko[1], G.P. Yablonskii[1], A.V. Mudryi[2], O.M. Borodavchenko[2], V.D. Zhivulko[2], R.W. Martin[3] and M.V. Yakushev [4,5,6]

[1] *Stepanov Institute of Physics, National Academy of Sciences of Belarus, Minsk, 220072 Belarus,*

[2] *Scientific-Practical Materials Research Centre, National Academy of Sciences of Belarus, Minsk, 220072 Belarus*

[3] *Department of Physics, SUPA, Strathclyde University, 107 Rottenrow, Glasgow, G4 0NG, UK*

[4] *M. N. Mikheev Institute of Metal Physics, UB RAS, Yekaterinburg, 620108 Russia*

[5] *Ural Federal University, Yekaterinburg, 620002 Russia*

[6] *Institute of Solid State Chemistry of the UB RAS, Ekaterinburg, 620990, Russia*

* michael.yakushev@strath.ac.uk

ABSTRACT

Excitonic quality $CuInSe_2$ crystals were studied using low-temperature (10 K) photoluminescence (PL) excited by continuous wave and nanosecond pulsed lasers at power densities from 0.01 kW/cm^2 to 76 kW/cm^2. Increasing the excitation power density level to 26 kW/cm^2 resulted in the appearance of a stimulated emission SE-band in the PL spectra at 1.035 eV. Further increase in the excitation level to 39 kW/cm^2 generated on the top of the SE band a structure of equidistant sharp lines attributed to laser emission.

Keywords: $CuInSe_2$, crystal, photoluminescence, pulsed laser excitation, stimulated emission, lasing

A direct bandgap of 1.05 eV and a high absorption coefficient in excess of 10^5 cm^{-1} make the semiconductor $CuInSe_2$ very attractive for applications in the absorber layer of thin films solar cells.[1,2] Solar cells with $Cu(In,Ga)Se_2$, (a compound derived from $CuInSe_2$ by admixing gallium) as the absorber layer is currently the leading thin film photovoltaic technology with respect to the conversion efficiency of laboratory size single junction devices, and stability. The conversion efficiency of such cells has already exceeded 23%.[3,4] This achievement makes $CuInSe_2$ a technologically important material. On the other hand, these properties along with excellent photostability suggest prospects for applications of $CuInSe_2$ as a laser material. Recent studies in this direction have demonstrated the possibility to achieve stimulated emission and lasing in $Cu(In,Ga)Se_2$ films at rather high doping levels (required for efficient solar cells).[5,6] However, the main physical processes involved in radiative recombination under high excitation intensity have not been clarified as yet. Understanding of such processes can provide an opportunity to develop a $CuInSe_2$-based near infrared diode laser.

Optical spectroscopy methods in general and photoluminescence (PL) in particular are amongst the most efficient experimental techniques used to examine the electronic properties of semiconductors.[7] PL, excited by high intensity pulsed lasers, can be used as an instrument to study nonequilibrium recombination processes of charge carriers.[8,9] Excitonic features, appearing in PL spectra at low concentrations of defects, make such spectra very informative.[10] Studies of excitonic quality $CuInSe_2$ and $Cu(In,Ga)Se_2$ thin films[2,11,12,13] as well as crystals[14,15] at low levels of continuous laser excitation demonstrate PL spectra with complicated patterns of free and bound excitonic lines. However, no PL studies of high quality $CuInSe_2$ crystals under high power density pulsed laser excitation can be found in the literature. Such studies can be expected to provide information on the processes nonequilibrium recombination of charge carriers in this compound, thus illuminating the main processes involved in radiative recombination.

In this paper we study the effect of high intensity nanosecond pulsed laser excitation on the near-band-edge PL spectra of excitonic quality $CuInSe_2$ crystals measured at 10 K.

Crystals of $CuInSe_2$ were freshly cleaved from the middle part of an ingot grown from a near stoichiometric charge of the high purity elements Cu, In, and Se by the vertical Bridgman technique.[16] The elemental composition of the crystals, measured by energy dispersive X-ray analysis (EDX) was close to the ideal stoichiometry Cu: 25.0 at.%, In: 24.9 at.%, and Se: 50.1 at. %.

Continuous laser excitation PL measurements were carried out at 5 K using the 514 nm line of an Ar^+ laser with an excitation power density of about 0.05 kW/cm^2. PL was collected by a concave mirror and focused on the slits of a 1 m single grating (600 grooves/mm) monochromator with a cooled InGaAs photomultiplier tube sensitive from 0.9 nm to 1.7 nm. Pulsed excitation PL measurements were carried out at 10 K. To expand the range of excitation intensities of the sample, two lasers were used: a semiconductor laser (λ = 435 nm, τ_p = 12 ns, f = 137 kHz, providing excitation power densities from 0.01 kW/cm^2 to 3.2 kW/cm^2) and a nitrogen laser (λ = 337.1 nm, τ_p = 8 ns, f = 525 Hz, with power density from 3.3 kW/cm^2 to 76 kW/cm^2). The laser beam, directed to the surface within 5 degrees from the normal, was focused on the surface of the samples into an area of 1 mm^2. The cleaved surface contained several micro-size steps (with one plane parallel whereas the other perpendicular to the surface) and cracks perpendicular to the surface. The power of the lasers was calculated as the ratio of the energy of one pulse to its full width at half maximum (FWHM). PL emission, collected by a lens in the direction close to the surface normal, was registered using a 0.3 m single grating (600 grooves/mm) monochromator and a linear array detector sensitive from 0.9 μm to 1.7 μm. For both continuous and pulsed excitation regimes the samples were cooled in a closed-cycle helium refrigerator. To improve cooling of the sample the crystal was immersed in an indium slab, which was then mounted on the cold finger.

Figure 1 shows a PL spectrum, measured at 5 K, excited by the continuous laser with power density of 0.05 kW/cm^2. This spectrum reveals two well resolved peaks at 1.042 eV and 1,045 eV, each with full width at half maximum of 1.5 meV. These peaks are the free A and B excitons,

respectively.[14,15] The spectrum also exhibits several sharp peaks M1, M2, M3, M5 and M6 with FWHMs of 0.5 meV, which are assigned to excitons bound to defects.[14] The figure compares this spectrum with one excited by the 435 nm line of the pulsed semiconductor laser with a power density of 0.06 kW/cm^2 and measured at 10 K. The two spectra demonstrate that the spectral position of the free and bound exciton lines coincides well.

The higher relative intensity of the M2 and M5 bound exciton peaks in the spectrum excited by the continuous laser can be explained by the lower temperature used during the acquisition of this spectrum whereas the near absence of the M1 and M3 peaks can be attributed to small differences in the elemental compositions of the areas excited by the continuous and pulsed lasers as well as by differences in the type of the excitation. Figure 2 shows the evolution of PL spectra (measured at 10 K) with excitation power density increasing from 0.01 to 3.2 kW/cm^2.

When the excitation power density increases above 0.17 kW/cm^2 a band, denoted as P-band, is generated at 1.037 eV. This band, with a FWHM of 5 meV, is much broader and grows faster than the excitonic lines resulting in a gradual disappearance of these lines from the spectra as shown in Figure 2. To quantify changes in the spectral position of this band with excitation power rise we fitted Lorentzian shapes into the M5, M6 narrow bound exciton lines and a broader Lorentzian at the low energy side of the spectra as shown in Figure 1(b). Under increasing excitation power the P-band gradually red shifts from 1.037 eV to 1.035 eV. Therefore, we make a preliminary assignment of this band as inelastic exciton-exciton scattering. Some excitons are scattered to an excited state whereas others decay with energy losses leading to the redshifted P-band (right band at 0.52 kW/cm^2 in Figure 2). Such bands were observed in the PL spectra of AlN [17] and ZnO[18] at intermediate excitation levels, at which excitonic lines are still present in the spectra but exciton-exciton interaction takes place.[19]

Further growth of the excitation power increases the FWHM of the P-band, which becomes 10 meV at an excitation of 2 kW/cm^2 suggesting the appearance of another band at 1.035 eV. This band, denoted as EHP, can be seen in Figure 2 merged with the P-band from the low energy side at

an excitation power density above 0.52 kW/cm^{-2}. We preliminary assign the EHP-band to radiative recombination of free charge carriers in an electron-hole plasma. Once the average distance between excitons becomes comparable to their Bohr radii the electrons and holes, excited to the conduction and valence bands, screen binding Coulomb forces between electrons and holes. Such screening weakens free excitons, reducing their binding energy, and releases bound excitons.[19] These processes are responsible for the gradual disappearance of excitonic lines from the spectra in Figure 2. The emission of an electron-hole plasma manifests itself in the spectra after the disappearance of exciton lines with an increase in the excitation level. Such an EHP-band also appeared in high excitation level PL spectra of AlN [17] and ZnO [18] at spectral energies just below that of the P-band. The further evolution of the PL spectra of $CuInSe_2$, excited by the pulsed nitrogen laser emission with power densities increasing from 3.3 kW/cm^2 to 76 kW/cm^2, is shown in Figure 3. At excitation power densities in excess of 20 kW/cm^2, another band at 1.032 eV, denoted as SE, becomes apparent on the low energy side of the EHP-band. We assign this band to stimulated emission. This band becomes dominant at power densities over 26 kW/cm^2. Figure 4(a) shows two Lorentzians fitted to the PL spectrum, measured at 26 kW/cm^2, to estimate the FWHM and spectral position of the SE band. Figure 4(b) presents the dependence of the integrated emission intensity from $CuInSe_2$ on the excitation power density on a logarithmic scale. The gradient of the straight line, fitted to the linear part of the data from 10 kW/cm^2 to 33 kW/cm^2, is close to $k = 2$, which supports the assignment of the recombination mechanism of the EHP band to electron-hole plasma. Figure 4(b) shows the FWHM of the SE band decreasing from 12 meV to 8 meV at the excitation power density growing from 20 kW/cm^2 to 40 kW/cm^2. This narrowing can be taken as a confirmation of the assignment of the recombination mechanism of the SE band to stimulated emission.[19]

At excitation power densities from 39 kW/cm^2, a structure of several sharp equidistant peaks appeared at the top of the SE-band indicating the onset of the laser emission regime. Together with the spectral narrowing of the SE band the appearance of the mode structure are characteristics of achieving the stimulated and laser emission regimes. The laser threshold pumping value, determined

by the linear extrapolation of the slope of the dependence, in the region of lasing is about 40 kW/cm^2. Changes in the shape of the PL spectra with increasing excitation power are also shown in Figure 5, where several spectra, selected from Figure 2 and Figure 3, and multiplied by individual constants chosen to fit these spectra to one figure to compare their shapes on a linear scale. Further increase in the excitation power demonstrates the growth of the SE-band intensity, narrowing of its peak and then the appearance of sharp lines at the peak maximum. Their sharpness and an explicit threshold character suggest the achievement of a lasing regime.

At high excitation levels, amplification is provided by recombination processes during interband transitions in a high-density electron-hole plasma. The spectral position of the gain spectrum is determined by the processes of renormalisation of the bandgap and band filling.[19]

The sharp line oscillation structure at the maximum of the SE-band and the equidistance of their spectral positions suggest that they can be formed in a simple two-mirror Fabry-Perot optical cavity. An additional confirmation of this origin of lasing is the stability of the spectral position of the oscillation structure lines with changes in the excitation intensity from 43 kW/cm^2 to 76 kW/cm^2 as shown in Figure 3 and Figure 5(b). This implies the presence in the excited region of the crystal of parallel micro-facets. We speculate, that such micro-facets, playing the role of cavity mirrors, can be formed by micro-cracks or grain boundaries perpendicular to the surface. Lasing from in-plane Fabry-Perot cavities, unintentionally formed by cracks in CdSe/ZnSe layers, and scattered into the vertical direction has previously been reported.[20]

If we neglect the dependence of the refractive index of $CuInSe_2$ on the wavelength, then from the interference condition for the generation of laser radiation in a simple Fabry-Perot two-mirror cavity we can determine the spectral distance between two adjacent maxima $\Delta\lambda = \lambda^2/2nl$, where λ is the lasing wavelength, n the refractive index of $CuInSe_2$ and l the laser cavity length. Hence, the cavity length can be estimated as $l \approx 240$ μm assuming $\lambda \approx 1.2$ μm, $\Delta\lambda \approx 1$ nm and $n \approx 3.0$,[21] which is in good agreement with the dimensions of the excitation laser spot on the sample surface.

After the high excitation measurements, the samples were re-examined using PL measurements at 5 K using continuous wave low power excitation. The observed PL spectra were very similar to those presented in Figure 1 suggesting that the samples were not damaged by the pulsed laser excitation.

In conclusion, emission spectra of excitonic quality $CuInSe_2$ crystals under nanosecond pulsed laser excitation with intensity ranging from 0.01 kW/cm^2 to 76 kW/cm^2 were studied at T=10 K. At low excitation levels the spectra showed radiative recombination of free and bound excitons. An increase in the excitation intensity over 0.5 kW/cm^2 resulted in the appearance in the spectra of an EHP-band at 1.035 eV, assigned to the recombination of non-equilibrium charge carriers in the electron-hole plasma. Further increase in the excitation level generated a stimulated emission SE-band at 1.033 eV and then several equidistant sharp lines manifesting the achievement of the lasing regime. The thresholds of the stimulated and laser emission regimes were 26 kW/cm^2 and 39 kW/cm^2, respectively. The regular mode structure (with equidistant longitudinal modes), could possibly be formed due to the presence in $CuInSe_2$ of parallel facets of microcracks or grain boundaries about 240 μm apart, which act as laser mirrors of the Fabry-Perot cavity.

This work was supported by State Program of Scientific Research of the Republic of Belarus "Physical Material Science, New Materials and Technologies" (Project no. 1.4.4) and Belarusian Republican Foundation of Basic Research (Grant no. F20M-058). The research was carried out within the state assignment of Ministry of Science and Higher Education of the Russian Federation ("Spin" No. AAAA-A18-118020290104-2).

DATA AVAILABILITY

The data that support the findings of this study are available from the corresponding author upon reasonable request.

REFERENCES

[1] M.V. Yakushev, F. Luckert, R.W. Martin, C. Faugeras, A.V. Karotki, and A.V. Mudryi, Jap. J. Appl. Phys. **50**, 05FC03 (2011).

[2] A.V. Mudryi, V.F. Gremenok, I. A. Victorov, V.B. Zalesski, F. V. Kurdesov, V.I. Kovalevski, M.V. Yakushev, R.W. Martin, Thin Solid Films, **431-432**, 193 (2003).

[3] M.A. Green, E.D. Dunlop, J. Hohl-Ebinger, M. Yoshita, N. Kopidakis, and X. Hao, Prog. Photovolt. Res. Appl., **28**, 3 (2020).

[4] M. Nakamura, K. Yamaguchi, Y. Kimoto, Y. Yasaki, T. Kato, H. Sugimoto. IEEE J. Photovolt., **9**, 1863 (2019).

[5] M. Moret, O. Briot, B. Gil, T. Lepetit, L. Arzel, and N. Barreau, Proc. of SPIE 9358, 93581A (2015).

[6] I.E. Svitsiankou, V.N. Pavlovskii, E.V. Lutsenko, G. P. Yablonskii, A. V. Mudryi, V. D. Zhivulko, M. V. Yakushev, and R.W. Martin, J. Phys. D: Appl. Phys. **49**, 095106 (2016).

[7] P.Y. Yu and M. Cardona, *Fundamentals of Semiconductors: Physics and Materials Properties* (Springer-Verlag, Berlin-Heidelberg, 2010).

[8] D. Kuciauskas, J.V. Li, M.A. Contreras, J. Pankow, P. Dippo, M. Young, L.M. Mansfield, R. Noufi, and D. Levi, J. Appl. Phys., **114**, 154505 (2013).

[9] M. Okano, Y. Takabayashi, T. Sakurai, K. Akimoto, H. Shibata, S. Niki, and Y. Kanemitsu, Phys. Rev. B **89**, 195203 (2014).

[10] E.H. Bogardus and H.B. Bebb, Phys. Rev. **176**, 993 (1968).

[11] S. Niki, H. Shibata, P.J. Fons, A. Yamada, A. Obara, Y. Makita, T. Kurafuji, S. Chichibu, H. Nakanishi, Appl. Phys. Lett. **67**, 1289 (1995).

[12] C. Spindler, F. Babbe, M. H. Wolter, F. Ehré, K. Santhosh, P. Hilgert, F. Werner, and S. Siebentritt, Phys. Rev. Mater. **3**, 090302 (2019).

[13] F. Babbe, H. Elanzeery, M. H. Wolter, K. Santhosh, and S. Siebentritt, J. Phys: Condens. Matter. **31**, 425702 (2019).

[14] F. Luckert, M.V. Yakushev, C. Faugeras, A.V. Karotki, A.V. Mudryi, and R.W. Martin, J. Appl. Phys. **111**, 093507 (2012).

[15] M. V. Yakushev, F. Luckert, A. V. Rodina, C. Faugeras, A. V. Karotki, A. V. Mudryi, and R. W. Martin, Appl. Phys. Lett. **101**, 262101 (2012).

[16] R D. Tomlinson, Solar Cells **16**, 17 (1986).

[17] M. Feneberg, R. A. R. Leute, B. Neuschl, K. Thonke, and M. Bickermann, Phys. Rev. B **82**, 075208 (2010).

[18] C. H. Chia, Y. J. Lai, T. C. Han, J. W. Chiou, Y. M. Hu, and W. C. Chou, Appl. Phys. Lett. **96**, 081903 (2010).

[19] C.F. Klingshirn, Semiconductor optics (Springer, 1997).

[20] D.M. Bagnall and K.P. O'Donnell, Appl. Phys. Lett. **68**, 3197 (1996).

[21] T. Kawashima, S. Adachi, H. Miyake, and K. Sugiyama, J. Appl. Phys. **84**, 5202 (1998).

FIG.1. PL spectra of $CuInSe_2$ (a) - excited by the continuous wave Ar^+ laser with a power density of 0.05 kW/cm^2 measured at 5 K (1, red line) and pulsed semiconductor laser with a power density of 0.06 kW/cm^2 measured at 10 K (2-black circles); (b) – PL spectrum of $CuInSe_2$ excited by pulsed semiconductor laser with a power density of 0.17 kW/cm^2 measured at 10 K (black squares) and fitted by three Lorentzian shapes: P-band, M5 and M6 bound excitons.

FIG.2. Evolution of the PL spectra of $CuInSe_2$ (measured at 10 K) excited by the pulsed semiconductor laser with power densities from 0.01 to 3.2 kW/cm^2.

FIG. 3. Evolution of the PL spectra of $CuInSe_2$ measured at 10 K and excited by the pulsed nitrogen laser with power densities from 3.3 to 76 kW/cm^2.

FIG. 4. An example of the decomposition of the PL spectrum, measured at a pulse excitation power of 26 kW/cm^2, using two Lorentzian shapes for the SE and EHP bands (a). Dependencies of the integral emission intensity from the sample (b to the left) and of the FWHM of the SE band (b to the right) on the pulsed excitation power density.

FIG. 5. Emission spectra of $CuInSe_2$, selected from Figure 2 and Figure 3, at pulsed lasers excitation with power densities from 0.06 to 43 kW/cm^2 (a). The relative intensities of these spectra were tuned to clarify changes in their shape and spectral position of the bands. Evolution of the oscillation structure lines at excitation power density increasing from 43 kW/cm^2 to 76 kW/cm^2 (b).

Fig.1

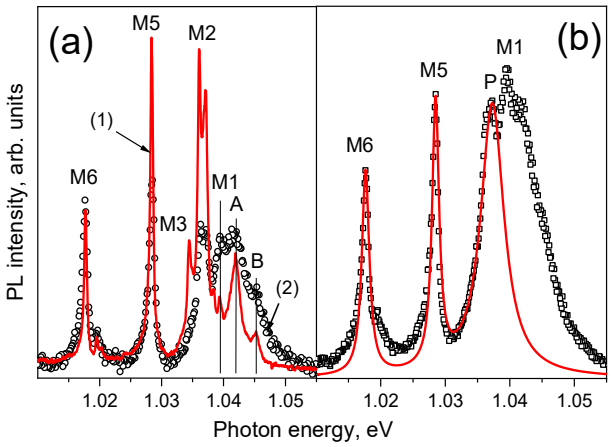
(a)
(b)
M5
M2
M1
M5
P
(1)
M6
M6
M1
A
M3
B
(2)
PL intensity, arb. units
1.02
1.03
1.04
1.05
1.02
1.03
1.04
1.05
Photon energy, eV

Fig. 2

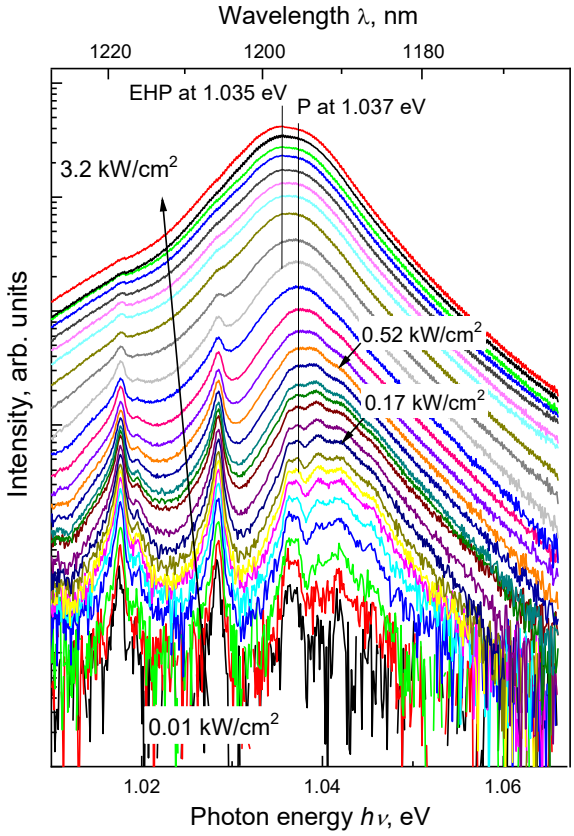
Wavelength λ, nm
1220
1200
1180
EHP at 1.035 eV
P at 1.037 eV
3.2 kW/cm2
0.52 kW/cm2
0.17 kW/cm2
0.01 kW/cm2
Intensity, arb. units
1.02
1.04
1.06
Photon energy hν, eV

Fig.3

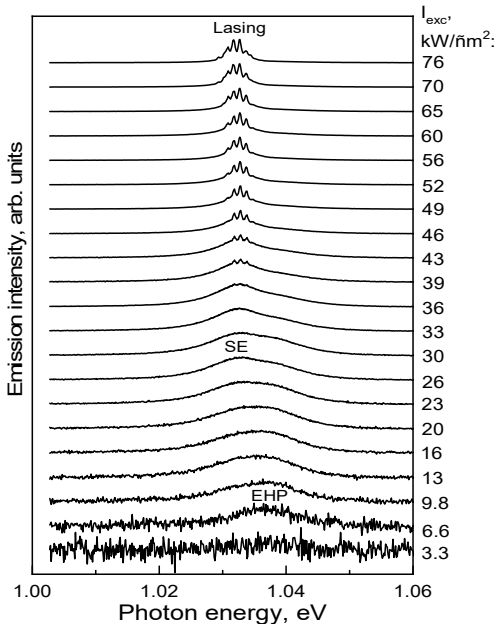
Lasing
SE
EHP
I_{exc}, kW/ñm^2:
76
70
65
60
56
52
49
46
43
39
36
33
30
26
23
20
16
13
9.8
6.6
3.3
Emission intensity, arb. units
1.00
1.02
1.04
1.06
Photon energy, eV

Fig.4

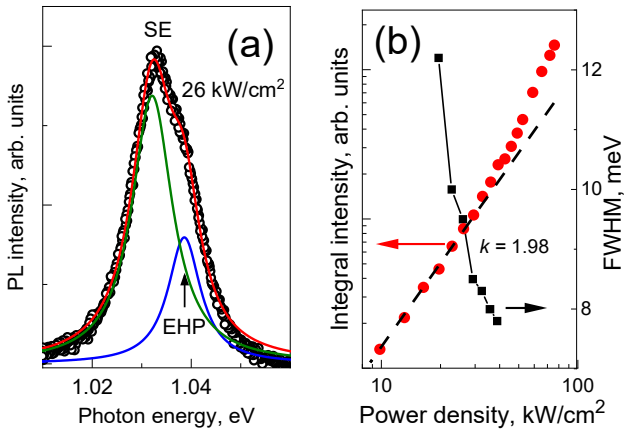
SE
(a)
26 kW/cm2
EHP
PL intensity, arb. units
1.02
1.04
Photon energy, eV
(b)
k = 1.98
Integral intensity, arb. units
FWHM, meV
12
10
8
10
100
Power density, kW/cm2

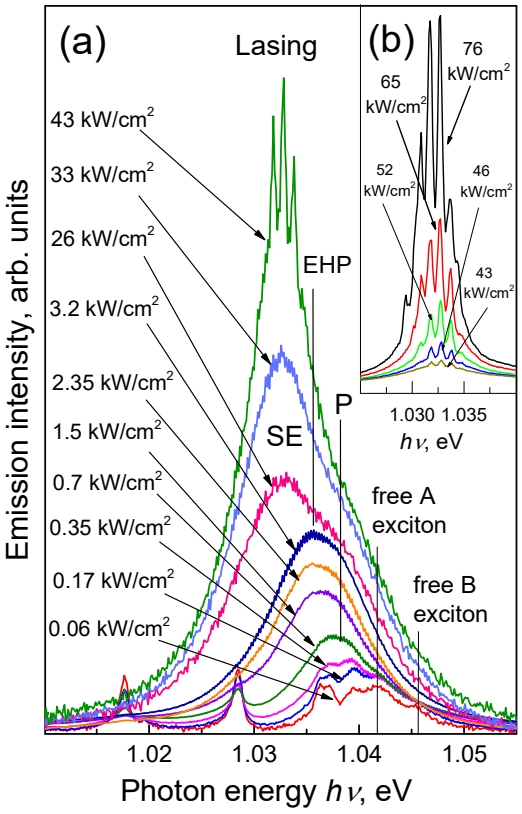
(a)
Lasing
(b)
76 kW/cm2
65 kW/cm2
52 kW/cm2
46 kW/cm2
43 kW/cm2
1.030 1.035
hν, eV
43 kW/cm2
33 kW/cm2
26 kW/cm2
3.2 kW/cm2
2.35 kW/cm2
1.5 kW/cm2
0.7 kW/cm2
0.35 kW/cm2
0.17 kW/cm2
0.06 kW/cm2
EHP
P
SE
free A exciton
free B exciton
Emission intensity, arb. units
1.02
1.03
1.04
1.05
Photon energy hν, eV